Intracellular Retention of Estradiol is Augmented by GRAM Domain Containing Protein ASTER-B in Breast Cancer Cells

Running Title:
ASTER-B Augments Intracellular E2 Levels

Hyung Bum Kim[1,2] and W. Lee Kraus[1,2,3,4]

[1] Laboratory of Signaling and Gene Regulation, Cecil H. and Ida Green Center for Reproductive Biology Sciences, University of Texas Southwestern Medical Center, Dallas, United States.

[2] Section of Laboratory Research, Department of Obstetrics and Gynecology, University of Texas Southwestern Medical Center, Dallas, United States.

[3] Address correspondence to: W. Lee Kraus (Lee.Kraus@utsouthwestern.edu)

[4]Lead Contact (for manuscript correspondence):
W. Lee Kraus, Ph.D.
Cecil H. and Ida Green Center for Reproductive Biology Sciences
The University of Texas Southwestern Medical Center at Dallas
5323 Harry Hines Boulevard, MC8511
Dallas, TX 75390-8511
Phone: 214-648-2388 / Fax: 214-648-0383
E-mail: Lee.Kraus@utsouthwestern.edu

Keywords: Estrogen receptor, E2, hormone, breast cancer, gene expression, ASTER-B

Funding: This work was supported by a grant from the NIH/National Institute of Diabetes and Digestive and Kidney Diseases (NIH/NIDDK; R01 DK069710) and funds from the Cecil H. and Ida Green Center for Reproductive Biology Sciences Endowment to W.L.K.

Disclosures: The authors have no relevant conflicts to disclose.

ABSTRACT

Estrogens are naturally occurring steroid hormones that also act as the primary mitogens for estrogen receptor-positive (ER+) breast cancers. While elevated blood levels of estrogens have been associated with poor prognosis, the relationship between circulating hormone levels in the blood are related to intracellular hormone concentrations. Here, we observed that MCF-7 cells acutely treated with 17β-estradiol (E2) retain a substantial amount of the hormone even upon removal of the hormone from the culture medium. Moreover, global patterns of E2-dependent gene expression are sustained for hours after acute E2 treatment and hormone removal. While circulating E2 is sequestered by sex hormone binding globulin (SHBG), the mechanisms of intracellular E2 retention are poorly understood. We found that a mislocalized GRAM-domain containing protein ASTER-B in the nucleus, which is observed in a subset of patients, is associated with higher cellular E2 retention. Accumulation and retention of hormone are related to the steroidal properties of E2. Finally, we observed that nuclear ASTER-B-mediated E2 retention is required for sustained hormone-induced ERα chromatin occupancy at enhancers and gene expression, as well as subsequent cell growth responses. Our results add intracellular hormone retention as a mechanism controlling E2-dependent gene expression and downstream biological outcomes.

SIGNIFICANCE

This study advances our understanding of how estradiol can be accumulated and retained intracellularly to drive a pro-proliferative gene expression program in ER+ breast cancer cells. Mechanistically, intracellular E2 retention is mediated in part by mislocalized, nuclear ASTER-B, which is aberrantly localized to the nuclei of cancer cells in some breast cancer patients.

INTRODUCTION

Estrogens are a class of steroid hormones required for a diverse range of physiological and pathological processes. The most abundant form, 17β-estradiol (E2), acts as the primary mitogen for estrogen receptor positive (ER+) breast cancer, which make up 80% of breast cancer molecular subtypes (1). Higher circulating concentrations of E2 are associated with a higher risk of breast cancer and a poorer patient outcome (2-4). Physiological levels of estrogens are regulated by their production, degradation, and sequestration (5). In fact, biological and pharmacological methods of reducing E2 levels have generally resulted in better prognosis. For example, inhibitors such as anastrozole, exemestane, or letrozole which target aromatases, key enzymes responsible for E2 production, effectively reduce circulating E2 concentrations, halting ER+ breast cancer growth and recurrence (6-9). In addition to its synthesis, circulating estrogens are bound by sex hormone binding globulin (SHBG), which binds and sequester steroid hormones, effectively limiting their bioavailability (10).

While the use of aromatase inhibitors has proven effective in reducing circulating E2 concentrations, intratumoral E2 concentrations are often elevated (11,12). Intratumoral concentrations of E2 have been found to be upwards of 10-fold higher than circulation concentrations (13). These elevated local concentrations have shown to facilitate growth of ER+ breast cancer despite reduced E2 in circulation. While aberrant intratumoral hormone production has been characterized, the role of cellular accumulation of E2 is still poorly understood (14,15). Therefore, mechanistic insight of E2 accumulation in breast cancer cells would be invaluable for better understanding effective E2 concentrations in ER+ BC.

Recently, ASTER-B has been implicated in E2 homeostasis. ASTER-B (encoded by *GRAMD1B*) is a GRAM-domain containing protein involved in nonvesicular cholesterol transport between the endoplasmic reticulum and plasma membrane. The protein is normally localized to the endoplasmic reticulum and has recently been shown to play a role in pathways involving estrogen production in the ovaries (16). Additionally, biochemical studies looking at binding affinities of a broad range of cholesterol-derived molecules show that ASTER-B can bind directly to E2, albeit with weak affinity (17). While these studies have begun to draw connections between ASTER-B and estrogen homeostasis, its role in ER+ breast cancer pathology has not been explored.

Here we characterize a novel association between ASTER-B and intercellular estrogen accumulation and retention. We show that the ER+ breast cancer cell line MCF-7 retains a significant amount of E2 intracellularly for a prolonged duration. Furthermore, we demonstrate that ASTER-B has aberrant nuclear localization in MCF-7 cells and that knockdown of ASTER-B greatly reduces E2 retention, its associated gene regulation, and its mitogenic effect.

RESULTS

Breast cancer cells retain intracellular E2 and sustain gene expression after acute E2 treatment followed by hormone washout

In order to determine the level of E2 cellular retention in ER+ breast cancer cells, MCF-7 cells were acutely treated with E2 followed by subsequent incubation in E2-free medium before measuring cellular E2 content (Fig. 1A). breast cancer cells lines expressing high ERα expression (MCF-7), moderate ERα expression (T-47D), and no ERα expression (MDA-MB-231) were tested. None of the cell lines had substantial E2 content prior to treatment. Both ER+ breast cancer cells lines accumulated a substantial level of E2, at a concentration similar to that of the treatment concentration. Moreover, MCF-7 cells retained almost half the treatment concentration of E2 after removal of the hormone from the medium, while T-47D and MDA-MB-231 have negligible intracellular E2 retention (Fig. 1B). In order to test whether retained E2 is conducive to signaling, we examined changes in gene expression. Remarkably, global gene expression was similar between conditions of continuous E2 treatment and washout conditions at least six hours post-treatment for both upregulated and downregulated genes (Fig. 1C). Furthermore, the total number of regulated genes in both continuously treated and washout conditions were similar for each timepoint (Fig. 1D and 1E), suggesting sustained E2 induction hours after removal of hormone from the culture medium.

To further determine how washout of hormone affects E2 induction over time, we categorized the into bins based on timepoint of maximum fold change expression over vehicle control (Bin 1 = 40 min., Bin 2 = 1 hr., Bin 3 = 2 hr., Bin 4 = 3 hr., and Bin 5 = 6 hr.). We observed that gene expression in bins 1 and 2 were lower in the washout condition as compared to continuous treatment (Fig. 2A and 2C). This was not observed at later time points. This suggests that genes with early induction are more sensitive to the removal of hormone. Furthermore, analysis of motifs near gene transcription start sites show changes in top motif usage across the bins, suggesting a link between induction time and sequence motif usage (Fig. 2B). In order to assess whether differences between sensitivity to hormone removal were due to a decrease in overall fold-change gene expression or overall change in number of genes, were determined induction levels and the fraction induced. Induction levels of the was determined as fraction of genes with induction levels in the washout at least 0.8-times that of continuous treatment across the bins. Induction levels of >0.8 were seen in each bin, indicating that genes are expressed in

washout groups to the same extent as the continuous treatment group (Fig. 2D). However, when assessing the relative number of genes in washout to continuous groups in each bin, fewer genes were present in bins 1 and 2 (Fig. 2D). Taken together, the differences between washout and continuous induction at the early timepoints (bins 1 and 2) were due to fewer number of induced genes in the washout groups rather than differences in the levels of gene expression.

Non-steroidal estrogen does not affect E2 accumulation or retention

Given that extracellular circulating steroid hormones are sequestered by SHBG, we hypothesized that intracellular E2 retention may also be working through its steroidal properties. Cells treated acutely with fluorescently labeled estradiol (E2-Glow) accumulated and retained a substantial amount of hormone intracellularly. Retained E2-Glow was resistant to washout with hormone-free medium for over 20 mins. (Fig. 3A). Additionally, unlabeled E2 efficiently competed intracellular E2-Glow, while the non-steroidal estrogen diethylstilbestrol (DES) failed to compete (Fig. 3B). This indicates that E2 accumulation and retention is due to its steroidal properties.

ASTER-B is mislocalized to the nucleus in both patient samples and MCF-7 cells

ASTER-B has been recently reported to be involved in E2 homeostasis (16). Promiscuous binding to cholesterol-derived molecules, including E2, has led us to investigate its role in intracellular E2 retention. ASTER-B is normally localized in the cytosol on the endoplasmic reticulum through its transmembrane domain. However, recent studies have shown that this protein is aberrantly translocated into the nucleus of certain gastric cancers (18). In fact, sequence analysis of ASTER-B using a publicly available prediction software (NovoPRO) shows a putative nuclear localization signal (NLS) C-terminal to the VASt/ASTdomain spanning amino acids 550-570 (Fig. 4A) (19).

Immunofluorescent staining of a panel of breast cancer cell lines (MCF-7, T-47D, MDA-MB-231) shows that MCF-7 cells have aberrantly localized nuclear ASTER-B, while T-47D and MDA-MB-231 have cytosolic ASTER-B (Fig. 4B). Additionally, examining RNA-seq data from the cancer genome atlas (TCGA) shows that high ASTER-B expression is associated with poor prognosis (overall survival) in luminal A breast cancer molecular subtype, which is ER+ and hormone responsive (Fig. 5A). Immunostaining using a commercial breast cancer tissue

microarray showed samples with either nuclear or cytoplasmic ASTER-B localization (Fig. 5B). Twenty-four out of 192 patients had nuclear localized ASTER-B, while 50 had cytoplasmic localization and 118 had no significant expression. Of the patients with nuclear ASTER-B localization, a majority (60.8%) were classified as invasive ductal carcinoma, followed by intraductal carcinoma (Fig. 5C). In contrast, patient samples with cytoplasmic ASTER-B consisted mostly of metastatic lesions (52%). Additionally, a higher proportion of samples with nuclear ASTER-B had high ERα expression as well as a higher proportion of stage III BC, as compared to cytosolic ASTER-B samples (Fig. 5D). Taken together, ASTER-B is found to be aberrantly localized to the nucleus in both patient samples and cultured cells. In patients, this is associated with both ERα expression and poorer prognosis.

GRAMD1B nuclear expression attenuates E2 cellular retention and gene regulation

Given ASTER-B's binding capacity for E2, we next explored whether its expression may be associated with hormone retention. *GRAMD1B* was knocked down using siRNA, leading to decreased ASTER-B protein expression (Fig. 6A and 6B). Knockdown of *GRAMD1B* in MCF-7 cells modestly decreased intracellular E2 accumulation. Moreover, E2 cellular retention after washout was dramatically decreased in *GRAMD1B* knockout (Fig. 6C and 6D). No changes in E2 levels were observed in the medium.

We next explored the effects of E2 retention on molecular features of E2 signaling. ERα chromatin occupancy at enhancer regions of E2 responsive genes (*P2RY2, NRIP1*) were maintained even after the washout of E2 from the culture medium (Fig. 6E). However, when *GRAMD1B* was knocked down, ERα chromatin occupancy was diminished only upon E2 washout. Furthermore, ERα binding reflected gene expression patterns, indicating that maintained cellular E2 is necessary for both sustained chromatin binding and gene expression (Fig. 6F). Moreover, we observed that E2 had a robust mitogenic effect on MCF-7 cells, with both continuous treatment and washout having significant proliferative effects (Fig. 6G). These effects were abrogated with *GRAMD1B* knockdown, with dampened growth observed with continuous E2 treatment and washout having a completely negligible effect on growth. Taken together, *GRAMD1B* was shown to support cellular accumulation and retention of E2, which is necessary to sustain gene regulatory programs upon hormone washout that modulate the mitogenic response.

DISCUSSION

In this study, we explored the association between a cholesterol binding protein, ASTER-B, and intracellular retention of E2. We showed that MCF-7 cells accumulate and retain E2 for a prolonged duration even after hormone removal. Retained E2 is associated with both sustained cell proliferation, as well as gene expression. We observed aberrant nuclear localization of ASTER-B in MCF-7 cells, which was associated with E2 retention, but not in other breast cancer cell lines. Aberrant nuclear localization of ASTER-B was also seen in tumor samples from a subset of breast cancer patients. We detected a modest association of ASTER-B nuclear expression with poor prognosis. Furthermore, knockdown of GRAMD1B lead to a significant decrease in cellular E2 retention as well as growth and gene regulatory programs, such as ERα binding and gene expression.

Mislocalization of ASTER-B leads to intracellular E2 retention

Little is known about how estrogen may be retained within the cell or how this may affect hormone-dependent gene regulation. We showed that acute treatment can support both cell proliferation as well as gene expression. Based on our genomic and cell-based assays, we find that ASTER-B mislocalization leads to increased intracellular E2 retention. This in turn supports ERα binding, gene expression, and cell proliferation for a prolonged duration after removal of E2 from the culture medium. While the mechanism of nuclear translocation of ASTER-B is not fully understood, it occurs in a variety of different pathologies, including gastrointestinal cancers and breast cancer (18). Initial analysis of COSMIC database shows mutations within the transmembrane domain of *GRAMD1B* that may allow for nuclear translocation through its cryptic NLS. Comparison between different breast cancer cell lines indicates that it is this nuclear localization of ASTER-B, and not necessarily its expression, that contributes to E2 retention.

Clinical implications of ASTER-B mislocalization

Analysis of tissue samples from ER+ breast cancer patients show a subset of patients with nuclear ASTER-B localization. These patients had a modest increase of both ERα expression as well as poorer prognosis. Combined with the cell-based assays performed in this study, these differences may be due to elevated E2 in the tumors of these patients. It is plausible that this may provide a growth advantage for ER+ breast cancer even in environments of fluctuating or low

estrogens. In fact, the highest instances of ER+ breast cancer are in postmenopausal women, where circulating E2 levels are greatly diminished (20).

ASTER-B supports E2-mediated gene regulation

We have demonstrated that hours after treatment, E2-regulated genes are expressed at the same fold-change intensity as continuous treatment. These effects are diminished, along with ERα binding, with the knockdown of ASTER-B and the reduction of intracellular E2. This implies that sustained induction by E2 is contingent on intracellularly available estrogen. Additionally, a recent study has shown that ASTER-B is involved in supporting E2 synthesis in the ovaries (16). Given its dual role in both estrogen production and intracellular retention, ASTER-B may be a potential therapeutic target that addresses multiple aspects of estrogen bioavailability.

METHODS

Antibodies

The custom rabbit polyclonal antiserum against ERα was generated, as previously described (21). The other antibodies used were as follows: rabbit polyclonal anti-GRAMD1B (ASTER-B) (Proteintech, 24905-1-AP; RRID:AB_2879791), mouse monoclonal anti-RPS6 (Santa Cruz, sc-74459; RRID:AB_1129205) and rabbit polyclonal anti-β-tubulin (Abcam, ab6046; RRID:AB_2210370).

Cell culture

MCF-7 cells were kindly provided by Dr. Benita Katzenellenbogen (University of Illinois at Urbana-Champaign, IL) and were maintained in minimal essential medium (MEM; Sigma M1018) supplemented with 5% calf serum (Sigma, C8056), 100 units/mL penicillin-streptomycin (Gibco, 15140122), and 25 µg/mL gentamicin (Gibco, 1571004). MDA-MB-231 cells were obtained from ATCC (HTB-26; RRID:CVCL_0062) and were maintained in Dulbecco's modified Eagle's medium- low glucose (DMEM; Sigma, D6046) supplemented with 10% fetal bovine serum (Sigma, F0926), 2 mM GlutaMAX (Gibco, 35050061), 100 units/mL penicillin-streptomycin (Gibco, 15140122), and 25 µg/mL gentamicin (Gibco, 1571004). T-47D cells were obtained from ATCC (HTB-133; RRID:CVCL_0553) and maintained in Roswell Park Medical Institute medium (RPMI; ThermoFisher, 11875119) supplemented with 10% fetal bovine serum (Sigma, F0926), 2 mM GlutaMAX (Gibco, 35050061), 100 units/mL penicillin-streptomycin (Gibco, 15140122), and 25 µg/mL gentamicin (Gibco, 1571004). All cell lines were authenticated for cell type identity using the GenePrint 24 system (Promega, B1870), and confirmed as *Mycoplasma*-free every six months using the Universal Mycoplasma Detection Kit (ATCC, 30-1012K). Fresh cell stocks were regularly replenished from original stocks every few months (no more than 10 passages).

Estradiol treatment and washout experiments

Seventy-two hours prior to E2 treatment, cells were cultured in hormone-free stripped medium consisting of Eagle's phenol red-free minimal essential medium (Sigma, M3024) supplemented with 5% charcoal-dextran treated calf serum (CDCS, Sigma, C8056), 2 mM GlutaMAX, 100 units/mL penicillin-streptomycin, and 25 µg/mL gentamicin. All subsequent

experiments involving E2 induction were carried out in stripped medium. For continuous induction experiments, cells were treated with DMSO (vehicle) or 100 nM 17β-estradiol (E2) (Sigma, E8875) for the indicated times. For washout experiments, cells were induced for 40 mins. with vehicle or 100 nM E2, washed once with stripped medium, then incubated in stripped medium for the remainder of the indicated time.

siRNA knockdown

For siRNA-mediated knockdown, siRNA against GRAMD1B (SASI_Hs02_0035373) or scramble siRNA (Sigma, SIC001) were purchased from Sigma and transfected into MCF-7 cells at a final concentration of 30 nM by electroporation using the SE Cell Line 4D-Nucleofector X kit (Lonza; EEID:SCR_023155). The cells were used for various assays 48 hours after siRNA transfection.

Measurement of E2 levels by ELISA

Treated cells and culture medium used for induction experiments were collected both before and after experimentation. In short, cells were harvested by washing once in ice cold 1X PBS and collected by scraping. Cells were then pelleted by centrifugation and packed cell volumes (PCV) were estimated. E2 was then extracted from samples by applying 5X volume (PCV or volume of medium) of pure methanol. Samples were vortexed for more than 30 seconds, then incubated at room temperature rotating end-over-end for 15 mins. Insoluble material was pelleted by centrifugation. The supernatant fraction was transferred to a new tube and dried in a vacuum desiccator. The resulting material was resuspended in appropriate volume of ELISA Buffer (provided by the Cayman Chemicals Estradiol ELISA kit). E2 concentrations were measured using the Estradiol ELISA kit (Cayman Chemicals, 501890) as described by the manufacturer's protocol.

Experiments with fluorescent E2

Stripped MCF-7 cells were seeded onto poly-lysine, γ-irradiated dishes (MatTek, P35GC-1/5-14-C) one day prior to imaging. Cells were treated with 100 nM Estradiol Glow (Jena Biosciences, PR-958S) for 20 mins at 37°C and images were acquired using an inverted Zeiss LSM 780 confocal microscope at 37°C and 5% CO_2. For washout experiments, preincubated cells were washed once with stripped medium, then incubated in stripped medium for the indicated

time. For competition assays, unlabeled 100 nM E2 or100 nM diethylstilbestrol (DES; Cayman Chemicals, 10006876) was added directly to the culture medium for the indicated time. Images were acquired using the Hamamatsu ORCA-Fusion C14440 digital camera and a CSU-W1 Yokogawa Spinning Disk Field Scanning Confocal System equipped with a Super Resolution by Optical Pixel Reassignment (SoRa) module. Images were acquired using a 20x Plan Apo Lambda objective (NA, 0.75) and a Z stack step size of 0.2 µm. Exposure time and laser intensity were kept consistent between samples. Laser lines 488 nm and 561 nm were used.

Identifying a putative NLS

The GRAMD1B amino acid sequence was analyzed using a publicly available software from NovoPRO (https://www.novoprolabs.com/tools/nls-signal-prediction) (19). ASTER-B protein sequence was analyzed using the two-state model preset, which uses a hidden Markov model to predict NLS. The top NLS signal with >90% probability was reported here.

Immunofluorescent staining

Breast cancer cells were seeded onto 4-well chambered slides (Thermo Fisher, 154917) one day prior to experimentation. The cells were washed once with PBS, fixed with 4% paraformaldehyde for 15 mins at room temperature, and washed three times with 1X PBS. The cells were permeabilized with 0.05% Triton X-100 in 1X PBS for 15 mins at room temperature, washed three times with PBS, and incubated for 1 hour at room temperature in Blocking Solution (1X PBS containing 1% BSA, 10% FBS, 0.3M glycine and 0.1% Tween-20). Fixed cells were incubated with a mixture of the primary antibodies in 1X PBS overnight at 4ºC, followed by three washes with PBS. The cells were then incubated with a mixture of Alexa Fluor 594 donkey anti-mouse IgG (ThermoFisher, A-21203; RRID:AB_2535789) and Alexa Fluor 488 goat anti-rabbit IgG (ThermoFisher, A-11008; RRID:AB_143165) each at a 1:500 dilution in 1X PBS for 1 hour at room temperature. After incubation, the cells were washed three times with 1X PBS. Finally, coverslips were placed on cells coated with VectaShield Antifade Mounting Medium with DAPI (Vector Laboratories, H-1200; RRID:AB2336790).

Immunocytochemistry staining of patient tumor microarray

A paraffin-embedded breast cancer patient tumor microarray was obtained from US

Biomax (BR2082b). Deparaffinization was performed by incubation in 100% xylene (Fisher, X3P) twice for 5 mins at room temperature. Slides were then rehydrated with sequential incubation in 100%, 95%, 70%, and 50% (Pharmco, 111000200) for 3 mins each at room temperature. Antigen retrieval was performed by incubation in boiling citrate buffer (10mM sodium citrate pH 6.0, 0.05% Tween-20) for 20 mins. Slides were then washed twice in 1X PBS for 10 mins at room temperature. Slides were blocked for 1 hour at room temperature using blocking solution described above, and stained for ASTER-B using a rabbit polyclonal antibody diluted 1:200 in 1X PBS for 2 hours at room temperature. Slides were then washed three times in 1X PBS, then incubated with Alexa Fluor 488 goat anti-rabbit IgG (ThermoFisher, A-11008; RRID:AB_143165) at a 1:500 dilution in 1X PBS for 1 hour at room temperature. Finally, coverslips were placed on cells coated with VectaShield Antifade Mounting Medium with DAPI (Vector Laboratories, H-1200; RRID:AB2336790).

Preparation of whole cell lysates

Cells were cultured and treated as described above before the preparation of cell extracts. At the conclusion of the treatments, the cells were washed twice with ice-cold 1X PBS and resuspended in lysis buffer (20 mM Tris-HCl pH 7.5, 150 mM NaCl, 1 mM EDTA, 1 mM EGTA, 1% NP-40, 1% sodium deoxycholate, 0.1% SDS) supplemented with 1 mM DTT and 1X complete protease inhibitor cocktail (Roche, 11697498001). The cells were incubated on ice in lysis buffer for 30 mins before vortexing followed by centrifugation at 20,000 g for 15 mins at 4°C in a microcentrifuge to remove the cell debris. Soluble material in the supernatant was collected for further processing.

Growth assay

Cells were maintained in stripped medium for 72 hours prior to growth assay. Cells were plated at a density of 50,000 cells per well in a 6-well dish. Cells were treated either continuously or acutely with washout as indicated above with 100 nM E2. At each 1 day timepoint, cells in a single well were trypsinized and live cell count obtained by staining with 0.4% trypan blue (Sigma, T8154) and counted using the BioRad TC20 automated cell counter. Culture medium was replenished every 2 days with 100 nM E2 for continuous treatment, or untreated stripped medium for washout conditions.

Immunoblotting

The protein concentrations of the cell lysates were determined using bicinchoninic acid (BCA) assay (Pierce, 23228). Volumes of lysates were adjusted to the same protein concentrations with lysis buffer and heated to 95°C for 5 mins after addition of appropriate amount of 4X SDS-PAGE Loading Solution (250 mM Tris, pH 6.8, 40% glycerol, 0.04% Bromophenol Blue, 4% SDS). Samples were run on polyacrylamide-SDS gels and transferred to nitrocellulose membranes. After blocking with 5% non-fat milk in TBS-T (50 mM Tris pH7.5, 150 mM NaCl, 0.1% Tween-20), the membranes were incubated with the primary antibodies described above in TBS-T with 0.02% sodium azide, followed by goat anti-rabbit HRP-conjugated secondary antibody at 1:5000 dilution (ThermoFisher, 31463; RRID:AB_228333). Immunoblot signals were detected using an ECL detection reagent (Thermo Fisher Scientific, 34577).

Reverse transcription quantitative PCR (RT-qPCR)

Breast cancer cells have undergone siRNA transfection and E2 treatment as described above. Total RNA was isolated using the Qiagen RNeasy Plus Mini kit (Qiagen, 74136) according to the manufacturer's protocol. Total RNA was reverse transcribed using oligo(dT) primers and MMLV reverse transcriptase (Promega, PR-M1705) to generate cDNA. The cDNA samples were subjected to RT-qPCR using gene-specific primers listed below. Target gene expression was normalized to the expression of GAPDH mRNA.

RT-qPCR primers

- GAPDH forward: 5’-CCACTCCTCCACCTTTGAC-3’
- GAPDH reverse: 5’-ACCCTGTTGCTGTAGCCA-3’
- GRAMD1B forward: 5’-GAGGAGAATGGAAACCAGAGCC-3’
- GRAMD1B reverse: 5’-GGTGAGGACTTCGGCATCTATC-3’
- P2RY2 forward: 5’-CGAGGACTTCAAGTACGTGCTG-3’
- P2RY2 reverse: 5’-GTGGACGCATTCCAGGTCTTGA-3’
- NRIP1 forward: 5’-GACCTGGCCCAGATAGATCA-3’
- NRIP1 reverse: 5’-TATAATGTAGGGGCGCAACC-3’

Chromatin immunoprecipitation quantitative PCR (ChIP-qPCR)

Chromatin immunoprecipitation (ChIP) was performed as previously described with some modifications (22). Cells were grown to ~80% confluence and treated as described above before crosslinking with 1% formaldehyde (ThermoScientific, 28-906) in 1X PBS at 37°C for 10 mins. The reaction was then quenched with glycine at a final concentration of 125 mM for 5 mins at 4°C. Cells were washed generously with ice-cold 1X PBS and collected by scraping with 1 mL ice-cold 1X PBS. The cells were pelleted by centrifugation and lysed by pipetting in Farnham Lysis Buffer (5 mM PIPES pH 8, 85 mM KCl, 0.5% NP-40, 1 mM DTT, 1X complete protease inhibitor cocktail). Nuclei were collected by brief centrifugation and resuspended in SDS Lysis Buffer (50 mM Tris-HCl pH 7.9, 1% SDS, 10 mM EDTA, 1 mM DTT, 1X complete protease inhibitor cocktail) by pipetting and incubating on ice for 10 mins. Chromatin was sheared to ~200–500 bp DNA fragments by sonication using a Bioruptor sonicator (Diagenode) for 8 cycles of 30 seconds on and 30 seconds off. Fragment size was verified by agarose gel electrophoresis before quantification of protein concentrations using BCA protein assay kit (Pierce, 23225). Samples were diluted 10-fold using dilution buffer (20 mM Tris-HCl pH 7.9, 0.5% Triton X-100, 2 mM EDTA, 150 mM NaCl) with freshly added 1mM DTT and 1X protease inhibitor cocktail. Soluble chromatin (500 µg per reaction) was precleared with Protein A Dynabeads (Invitrogen, 10001D). Protein A Dynabeads were incubated with 10 µL of polyclonal antiserum for ERα or 5 µg of rabbit IgG control (ThermoFisher, 10500C; RRID:AB_2532981) for 2 hours, washed with dilution buffer, and applied separately to precleared chromatin samples.

The immune complexes from the ChIP were washed once with each of the following in order: (1) low salt [20 mM Tris-HCl pH 7.9, 2 mM EDTA, 125 mM NaCl, 0.05% SDS, 1% Triton X-100, 1X complete protease inhibitor cocktail]; (2) high salt [20 mM Tris-HCl pH 7.9, 2 mM EDTA, 500 mM NaCl, 0.05% SDS, 1% Triton X-100, 1X complete protease inhibitor cocktail]; (3) LiCl [20 mM Tris-HCl pH 7.9, 1 mM EDTA, 250 mM LiCl, 1% NP-40, 1% sodium deoxycholate, 1X complete protease inhibitor cocktail]; (4) 1X Tris-EDTA [TE] containing 1X complete protease inhibitor cocktail. The precipitated immune complexes were transferred to a new tube in 1X TE before incubation in Elution Buffer (100 mM NaHCO3, 1% SDS) overnight at 65°C to de-crosslink and elute. Eluates were treated with DNase-free RNase (Roche, 11119915001) for 30 mins at 37°C, followed by 50 µg proteinase K (Life Technologies, 2542) for 2 hours at 55°C. Genomic DNA was purified by phenol chloroform extraction as previously

described (23). ChIPed DNA was analyzed by qPCR. Non-specific background signals were determined using rabbit IgG isotype ChIP. The data were expressed as percent input.

ChIP-qPCR primers

- P2RY2 enh. forward: 5'-AGGTAAGAGCTGAGGAGCCC-3'
- P2RY2 enh. reverse: 5'-CTTGACACCCCCAAGTGAGT-3'
- NRIP1 forward: 5'-GGCAGGTGATGATAACTCTGTAAGAAACC-3'
- NRIP1 reverse: 5'-GACAAACTGAACTTCTATACAGAGCTGCT-3'

RNA-sequencing

RNA-seq libraries were generated as previously described with the following modifications (24). Total RNA from MCF-7 cells treated as indicated was isolated using the Qiagen RNeasy Plus Mini kit (Qiagen, 74136) according to the manufacturer's protocol. Total RNA was then enriched for mRNA using Dynabeads Oligo(dT)25 (Invitrogen, 61002). Further fragmentation, first-strand cDNA synthesis, and subsequent procedures have been done as described (25).The libraries were subjected to quality control analyses, such as optimizing the number of PCR cycles required to amplify each set of libraries, quantifying the final library yield by Qubit fluorometer (Invitrogen, Q32851), and checking the size distribution of the final library by DNA ScreenTape system (Agilent Technologies, G2964AA, 5067–5584, and 5067–5603). The libraries were barcoded with indices as described for the Illumina TruSeq RNA Prep kit, multiplexed, and sequenced using Illumina NextSeq (2000) by 100 bp single-end sequencing. The RNA-seq data has been has been submitted to NCBI GEO. The accession number will be provided when available.

Analysis of RNA-seq data

The following steps were used to analyze the RNA-seq data: (1) Raw data was analyzed using FastQC tool for quality control; (2) Paired-end total RNA-seq reads were aligned to the human reference genome (GRCh38/hg38) using Star with default parameters; (3) Output files were then converted into BED files using SAMtools and BEDtools; and (4) bigWig files for visualization were generated using BEDtools. Heatmaps were generated using Java TreeView

(26,27). Motif analysis was done using HOMER gene-based analysis and ranked based on p-values (28).

Quantification and statistical analyses

All sequencing-based genomic experiments were performed a minimum of two times with independent biological samples. Statistical analyses for the genomic experiments were performed using standard genomic statistical tests as described above. All gene specific qPCR-based experiments were performed a minimum of three times with independent biological samples. Statistical analyses were performed using GraphPad Prism 9. All tests and p-values are provided in the corresponding figures or figure legends.

Data availability statement

All data generated in this study are available upon request from the corresponding author. The RNA-seq data has been submitted to NCBI GEO. The accession number will be provided when available.

DISCLOSURES

The authors have no relevant conflicts to disclose.

AUTHOR CONTRIBUTIONS

H.B.K.: Conceptualization, formal analysis, methodology, investigation, visualization, validation, writing-original draft. W.L.K.: Conceptualization, project development, funding acquisition, supervision, methodology, validation, project administration, visualization, writing-final draft.

ACKNOWLEDGEMENTS

We would like to acknowledge Tulip Nandu for help in the computational analysis of RNA-seq data, Cristel Camacho for critical review of the manuscript, and Mikayla Stokes for scientific discussions. This work was supported by grants from the NIH/National Institute of Diabetes and Digestive and Kidney Diseases (NIH/NIDDK; R01 DK069710) and funds from the Cecil H. and Ida Green Center for Reproductive Biology Sciences Endowment to W.L.K.

NOTE

This article contains no supplementary data.

REFERENCES

1. Hanker AB, Sudhan DR, Arteaga CL. Overcoming Endocrine Resistance in Breast Cancer. Cancer Cell **2020**;37(4):496-513 doi 10.1016/j.ccell.2020.03.009.

2. Endogenous H, Breast Cancer Collaborative G, Key TJ, Appleby PN, Reeves GK, Travis RC*, et al.* Sex hormones and risk of breast cancer in premenopausal women: a collaborative reanalysis of individual participant data from seven prospective studies. Lancet Oncol **2013**;14(10):1009-19 doi 10.1016/S1470-2045(13)70301-2.

3. Zhang X, Tworoger SS, Eliassen AH, Hankinson SE. Postmenopausal plasma sex hormone levels and breast cancer risk over 20 years of follow-up. Breast Cancer Res Treat **2013**;137(3):883-92 doi 10.1007/s10549-012-2391-z.

4. Pan H, Gray R, Braybrooke J, Davies C, Taylor C, McGale P*, et al.* 20-Year Risks of Breast-Cancer Recurrence after Stopping Endocrine Therapy at 5 Years. N Engl J Med **2017**;377(19):1836-46 doi 10.1056/NEJMoa1701830.

5. Nelson LR, Bulun SE. Estrogen production and action. J Am Acad Dermatol **2001**;45(3 Suppl):S116-24 doi 10.1067/mjd.2001.117432.

6. Chumsri S, Howes T, Bao T, Sabnis G, Brodie A. Aromatase, aromatase inhibitors, and breast cancer. J Steroid Biochem Mol Biol **2011**;125(1-2):13-22 doi 10.1016/j.jsbmb.2011.02.001.

7. Cuzick J, Sestak I, Baum M, Buzdar A, Howell A, Dowsett M*, et al.* Effect of anastrozole and tamoxifen as adjuvant treatment for early-stage breast cancer: 10-year analysis of the ATAC trial. Lancet Oncol **2010**;11(12):1135-41 doi 10.1016/S1470-2045(10)70257-6.

8. Morden JP, Alvarez I, Bertelli G, Coates AS, Coleman R, Fallowfield L*, et al.* Long-Term Follow-Up of the Intergroup Exemestane Study. J Clin Oncol **2017**;35(22):2507-14 doi 10.1200/JCO.2016.70.5640.

9. Carlson RW, Hudis CA, Pritchard KI, National Comprehensive Cancer Network Breast Cancer Clinical Practice Guidelines in O, American Society of Clinical Oncology Technology Assessment on the Use of Aromatase I, St Gallen International Expert Consensus on the Primary Therapy of Early Breast C. Adjuvant endocrine therapy in hormone receptor-

positive postmenopausal breast cancer: evolution of NCCN, ASCO, and St Gallen recommendations. J Natl Compr Canc Netw **2006**;4(10):971-9 doi 10.6004/jnccn.2006.0082.

10. Fortunati N, Catalano MG, Boccuzzi G, Frairia R. Sex Hormone-Binding Globulin (SHBG), estradiol and breast cancer. Mol Cell Endocrinol **2010**;316(1):86-92 doi 10.1016/j.mce.2009.09.012.

11. Haynes BP, Straume AH, Geisler J, A'Hern R, Helle H, Smith IE*, et al.* Intratumoral estrogen disposition in breast cancer. Clin Cancer Res **2010**;16(6):1790-801 doi 10.1158/1078-0432.CCR-09-2481.

12. Takagi K, Ishida T, Miki Y, Hirakawa H, Kakugawa Y, Amano G*, et al.* Intratumoral concentration of estrogens and clinicopathological changes in ductal carcinoma in situ following aromatase inhibitor letrozole treatment. Br J Cancer **2013**;109(1):100-8 doi 10.1038/bjc.2013.284.

13. van Landeghem AA, Poortman J, Nabuurs M, Thijssen JH. Endogenous concentration and subcellular distribution of estrogens in normal and malignant human breast tissue. Cancer Res **1985**;45(6):2900-6.

14. Suzuki T, Miki Y, Ohuchi N, Sasano H. Intratumoral estrogen production in breast carcinoma: significance of aromatase. Breast Cancer **2008**;15(4):270-7 doi 10.1007/s12282-008-0062-z.

15. Takagi M, Miki Y, Miyashita M, Hata S, Yoda T, Hirakawa H*, et al.* Intratumoral estrogen production and actions in luminal A type invasive lobular and ductal carcinomas. Breast Cancer Res Treat **2016**;156(1):45-55 doi 10.1007/s10549-016-3739-6.

16. Xiao X, Kennelly JP, Feng AC, Cheng L, Romartinez-Alonso B, Bedard A*, et al.* Aster-B-dependent estradiol synthesis protects female mice from diet-induced obesity. J Clin Invest **2024**;134(4) doi 10.1172/JCI173002.

17. Sandhu J, Li S, Fairall L, Pfisterer SG, Gurnett JE, Xiao X*, et al.* Aster Proteins Facilitate Nonvesicular Plasma Membrane to ER Cholesterol Transport in Mammalian Cells. Cell **2018**;175(2):514-29 e20 doi 10.1016/j.cell.2018.08.033.

18. Khanna P, Chua PJ, Wong BSE, Yin C, Thike AA, Wan WK*, et al.* GRAM domain-containing protein 1B (GRAMD1B), a novel component of the JAK/STAT signaling pathway, functions in gastric carcinogenesis. Oncotarget **2017**;8(70):115370-83 doi 10.18632/oncotarget.23265.

19. Nguyen Ba AN, Pogoutse A, Provart N, Moses AM. NLStradamus: a simple Hidden Markov Model for nuclear localization signal prediction. BMC Bioinformatics **2009**;10:202 doi 10.1186/1471-2105-10-202.

20. Murase K, Yanai A, Saito M, Imamura M, Miyagawa Y, Takatsuka Y*, et al.* Biological characteristics of luminal subtypes in pre- and postmenopausal estrogen receptor-positive and HER2-negative breast cancers. Breast Cancer **2014**;21(1):52-7 doi 10.1007/s12282-012-0348-z.

21. Kraus WL, Kadonaga JT. p300 and estrogen receptor cooperatively activate transcription via differential enhancement of initiation and reinitiation. Genes Dev **1998**;12(3):331-42 doi 10.1101/gad.12.3.331.

22. Murakami S, Nagari A, Kraus WL. Dynamic assembly and activation of estrogen receptor alpha enhancers through coregulator switching. Genes Dev **2017**;31(15):1535-48 doi 10.1101/gad.302182.117.

23. Murakami S, Li R, Nagari A, Chae M, Camacho CV, Kraus WL. Distinct Roles for BET Family Members in Estrogen Receptor alpha Enhancer Function and Gene Regulation in Breast Cancer Cells. Mol Cancer Res **2019**;17(12):2356-68 doi 10.1158/1541-7786.MCR-19-0393.

24. Hou TY, Kraus WL. Analysis of estrogen-regulated enhancer RNAs identifies a functional motif required for enhancer assembly and gene expression. Cell Rep **2022**;39(11):110944 doi 10.1016/j.celrep.2022.110944.

25. Zhong S, Joung JG, Zheng Y, Chen YR, Liu B, Shao Y*, et al.* High-throughput illumina strand-specific RNA sequencing library preparation. Cold Spring Harb Protoc **2011**;2011(8):940-9 doi 10.1101/pdb.prot5652.

26. Saldanha AJ. Java Treeview--extensible visualization of microarray data. Bioinformatics **2004**;20(17):3246-8 doi 10.1093/bioinformatics/bth349.

27. Dobin A, Davis CA, Schlesinger F, Drenkow J, Zaleski C, Jha S*, et al.* STAR: ultrafast universal RNA-seq aligner. Bioinformatics **2013**;29(1):15-21 doi 10.1093/bioinformatics/bts635.

28. Heinz S, Benner C, Spann N, Bertolino E, Lin YC, Laslo P*, et al.* Simple combinations of lineage-determining transcription factors prime cis-regulatory elements required for macrophage and B cell identities. Mol Cell **2010**;38(4):576-89 doi 10.1016/j.molcel.2010.05.004.

FIGURE LEGENDS

Figure 1. Intracellular E2 retention in MCF-7 cells is associated with sustained gene expression after hormone removal.

(A) Schematic showing workflow of induction and washout experiments.

(B) Cellular E2 levels of breast cancer cell lines including MCF-7, T-47D, and MDA-MB-231 as measured by an ELISA-based assay. Fraction of E2 retained in cells were calculated by dividing measured E2 levels in the washout conditions with their respective E2 treated conditions. Significance was determined using multiple Student's t-tests (non-parametric) with a Šidák-Bonferroni correction. p-values are indicated, n = 3.

(C) Heatmap showing fold-change gene expression derived from RNA-seq for continuous treatment and washout experiments. Timepoints indicate the duration of experimentation. Genes are ranked based on fold change at endpoint (360 mins) of continuous treatment conditions.

(D) Venn diagrams showing the overlap of all differentially expressed genes between the continuous treatment and washout conditions for both upregulated (*left panel*) and downregulated (*right panel*) genes.

(E) Graph showing relative reads per kilobase mapped reads (RPKM) for continuous treatment and washout conditions across different timepoints for upregulated (*left panel*) and downregulated (*right panel*) genes.

Figure 2. Analysis of steady-state gene expression upon continuous E2 treatments or after washout.

(A) Bins showing relative number of genes grouped based on time of maximum expression for both continuous and washout groups (Bin 1 = 40 min., Bin 2 = 1 hr., Bin 3 = 2 hr., Bin 4 = 3 hr., and Bin 5 = 6 hr.). Solid lines represent continuous treatment and dotted lines represent washout treatment.

(B) Top motif found within 500 bp of gene transcription start sites for each bin. P-values are shown below motif logos.

(C) Browser tracks of representative genes for each bin. From left to right black = Bin 1, red = Bin 2, green = Bin 3, blue = Bin 4, and purple = Bin 5. Darker colors represent continuous treatment and lighter colors represent washout treatment.

(D) Graphs showing induction levels calculated by relative number of genes in washout group with fold-change induction >0.8 that of continuous treatment groups for each bin or fraction of genes induced calculated by the ratio of genes in the washout to continuous treatment that have fold-change induction >1.5.

Figure 3. Washout and competition analyses of E2 retention in MCF-7 cells.

(A) Washout with hormone-free stripped medium after acute treatment with 100 nM E2-Glow reagent. Quantification of relative intensity of washout experiment images from n = 3 independent biological replicates normalized to value at t = 0 mins (time of washout). The scale is indicated.

(B) Competition with 100X concentration of unlabeled E2 (*top panel*) or 100X DES (*bottom panel*) after acute treatment with 100 nM E2-Glow. Quantification of competition experiment images from n = 3 independent biological replicates normalized to value at t = 0 mins (time after addition of unlabeled E2 or DES). The scale is indicated.

Figure 4. ASTER-B localization in breast cancer cells.

(A) Schematic showing the domain structure of ASTER-B protein. Putative nuclear localization signal (NLS) is highlighted in red along with its sequence.

(B) Immunofluorescence images of breast cancer cell lines stained for ASTER-B (*green*), RPS6 endoplasmic reticulum stain (*red*), and DAPI nuclear stain (*blue*). The scale is indicated.

Figure 5. Nuclear ASTER-B localization is associated with decreased survival.

(A) Kaplan-Meier survival plots of all TCGA breast cancer patients (n = 1064; *left panel*) and specifically luminal A subtype breast cancer patients (n = 415; *right panel*) with high (*red line*) or low (*blue line*) GRAMD1B expression level over a 5-year period. P-values calculated using the Log-rank test.

(B) Representative images of either nuclear (*top panel*) or cytoplasmic (*bottom panel*) ASTER-B (*green*) co-stained with DAPI (*blue*).

(C) Pie charts showing the histological subtypes of patients with either nuclear localized (*left panel*) or cytoplasmic (*right panel*) ASTER-B as assessed by immunostaining of a commercial breast cancer tissue microarray.

(D) Graphs showing ERα expression status (*left panel*) and breast cancer stages (*right panel*) of nuclear or cytoplasmic ASTER-B in a breast cancer tissue microarray as determined by immunohistochemistry (IHC) staining and histology respectively.

Figure 6. ASTER-B nuclear localization is associated with cellular retention of E2, regulation of gene expression, and growth in MCF-7 cells.

(A and B) Western blot (A) and immunofluorescence images (B) showing knockdown of ASTER-B in MCF-7 cells. The scale in panel B is indicated.

(C and D) Measurement of intracellular (*left panel*) and culture medium (*right panel*) E2 levels by ELISA-based quantification. In panel D, significance was determined using multiple Student's t-tests (non-parametric) with a Šidák-Bonferroni correction. The p-value is indicated, n = 3.

(E and F) Chromatin occupancy of ERα at enhancer regions and its corresponding gene expression at E2 regulated genes (*P2RY2* and *NRIP1*) measured by ERα ChIP-qPCR and RT-qPCR respectively. For statistical analysis, comparisons were made against vehicle control for their own treatment groups. Multiple Student's unpaired t-tests (non-parametric) with a Šidák-Bonferroni correction used to determine significance. Significance values were assigned as follows: * $p<0.033$, ** $p<0.002$, *** $p<0.0001$, **** $p<0.00001$. n = 3.

(G) Growth assay of cells treated continuously with 100 nM E2, or treated acutely for 40 mins on day one (washout), or treated with vehicle control. MCF-7 cells were treated with control siRNA (*left panel*) or siGRAMD1B (*right panel*). Multiple Student's unpaired t-tests (non-parametric) with a Šidák-Bonferroni correction used to determine significance. Significance values were assigned as follows: * $p<0.033$, ** $p<0.002$, *** $p<0.0001$, **** $p<0.00001$. n = 3.

Figure 7. ASTER-B augments intracellular retention of E2 and supports biological outcomes in breast cancer cells.

(A and B) Schematic showing a working model of ASTER-B mediated E2 cellular retention. Figures were generated using BioRender (BioRender.com). Details are provided in the text.

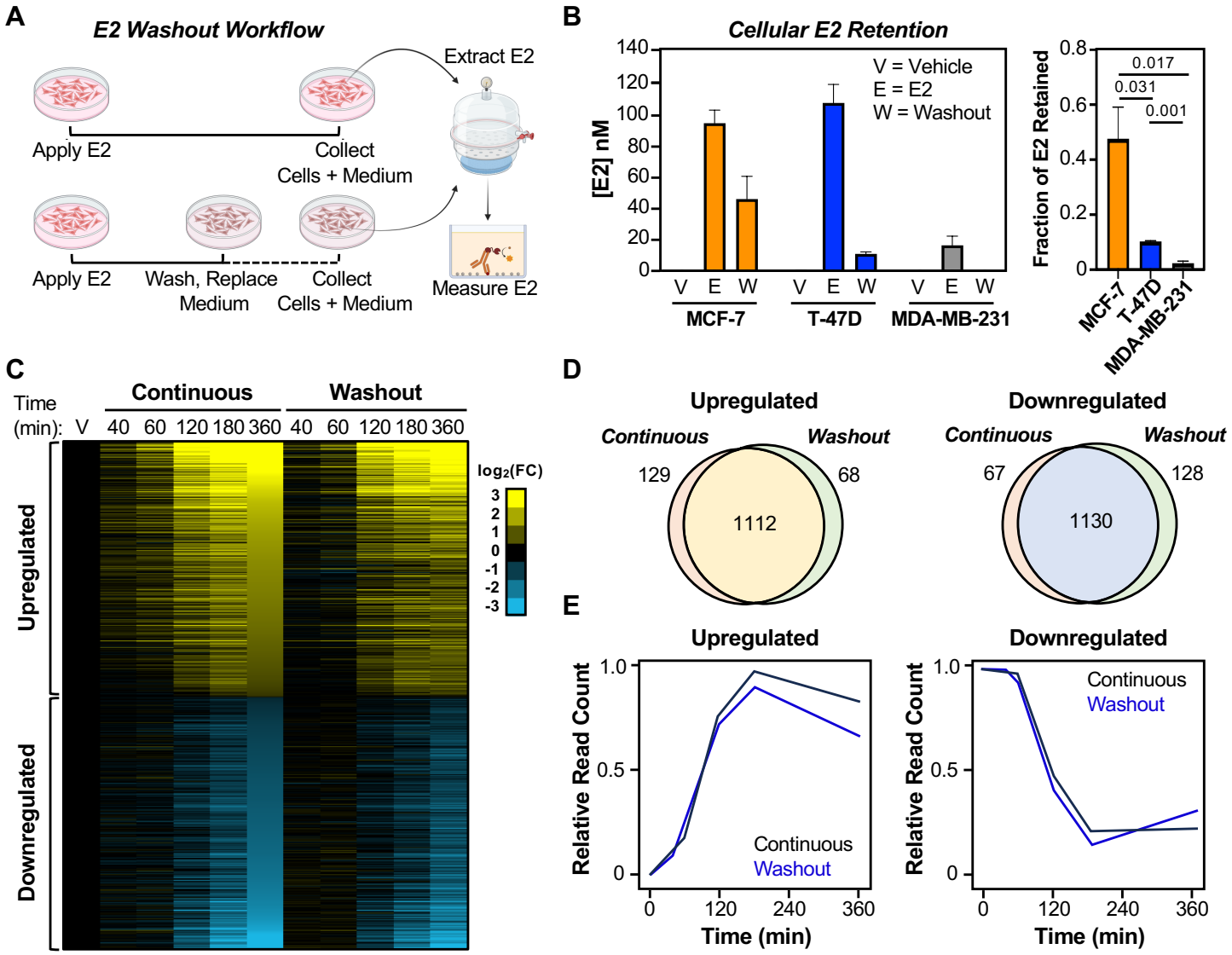

Kim and Kraus (2024) - Figure 1

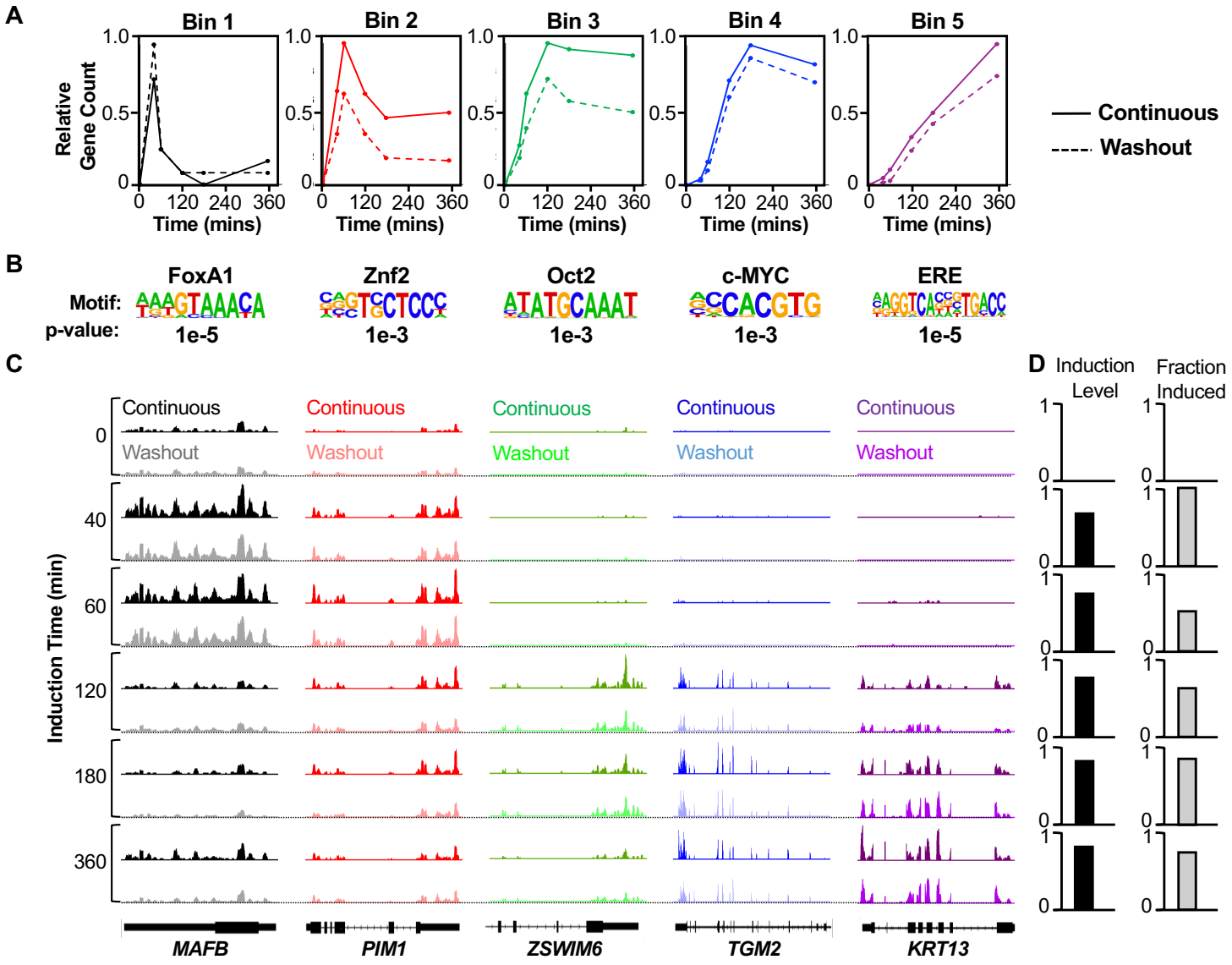

Kim and Kraus (2024) - Figure 2

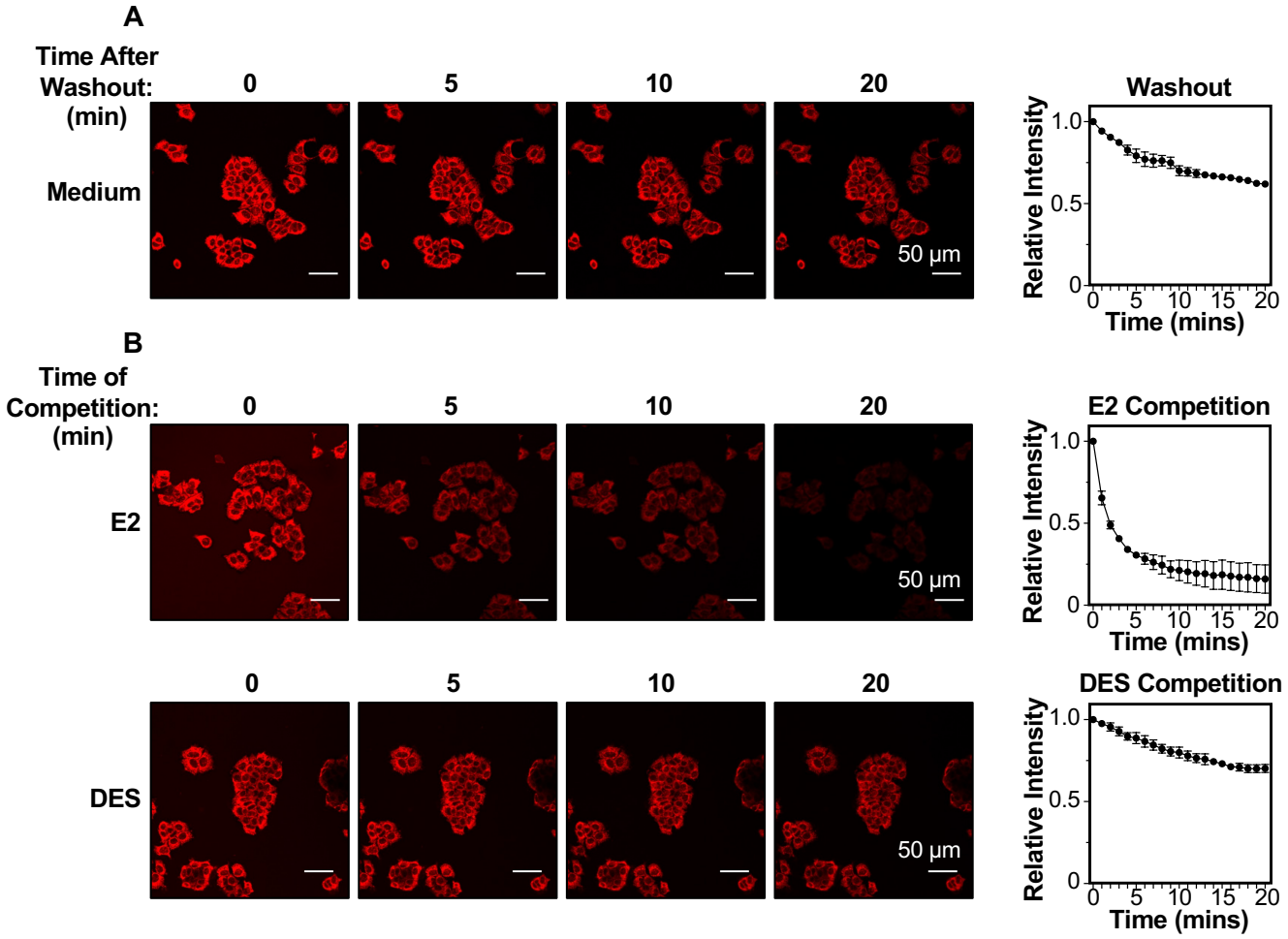

Kim and Kraus (2024) - Figure 3

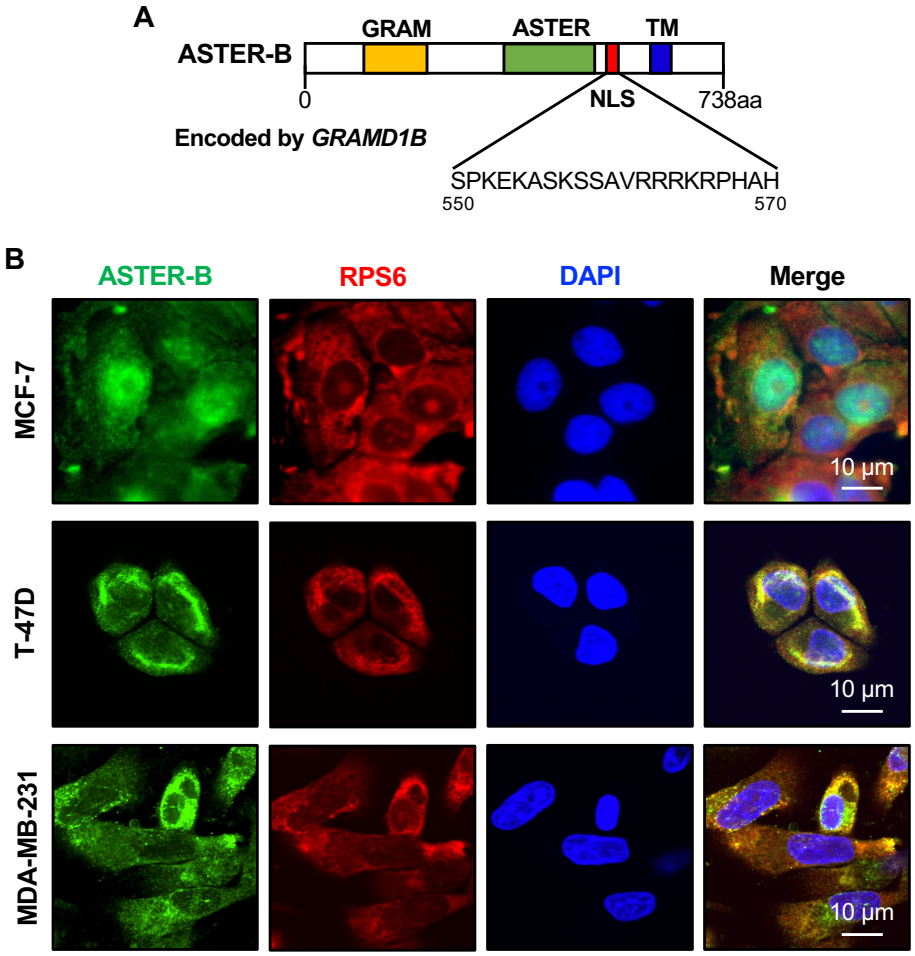

Kim and Kraus (2024) - Figure 4

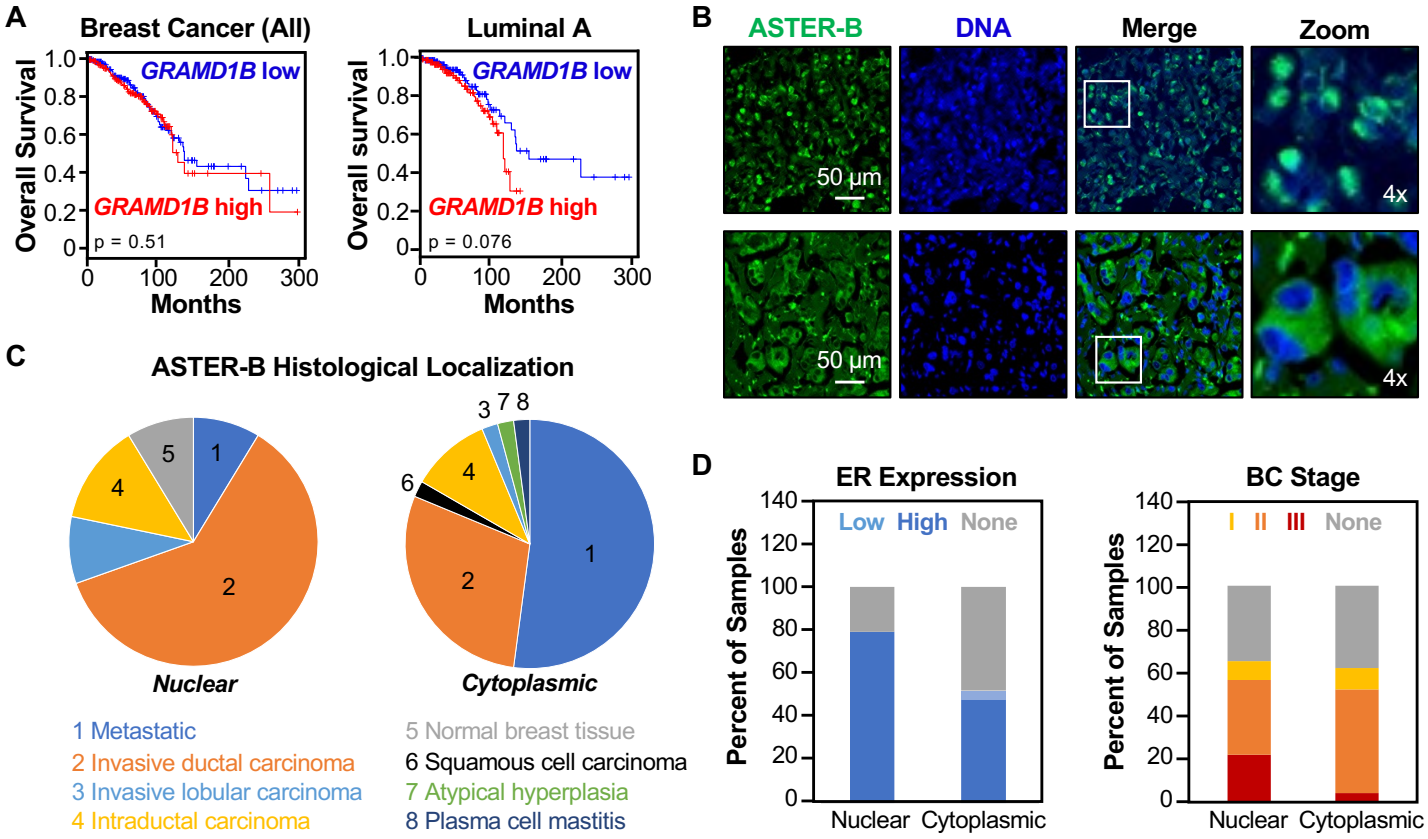

Kim and Kraus (2024) - Figure 5

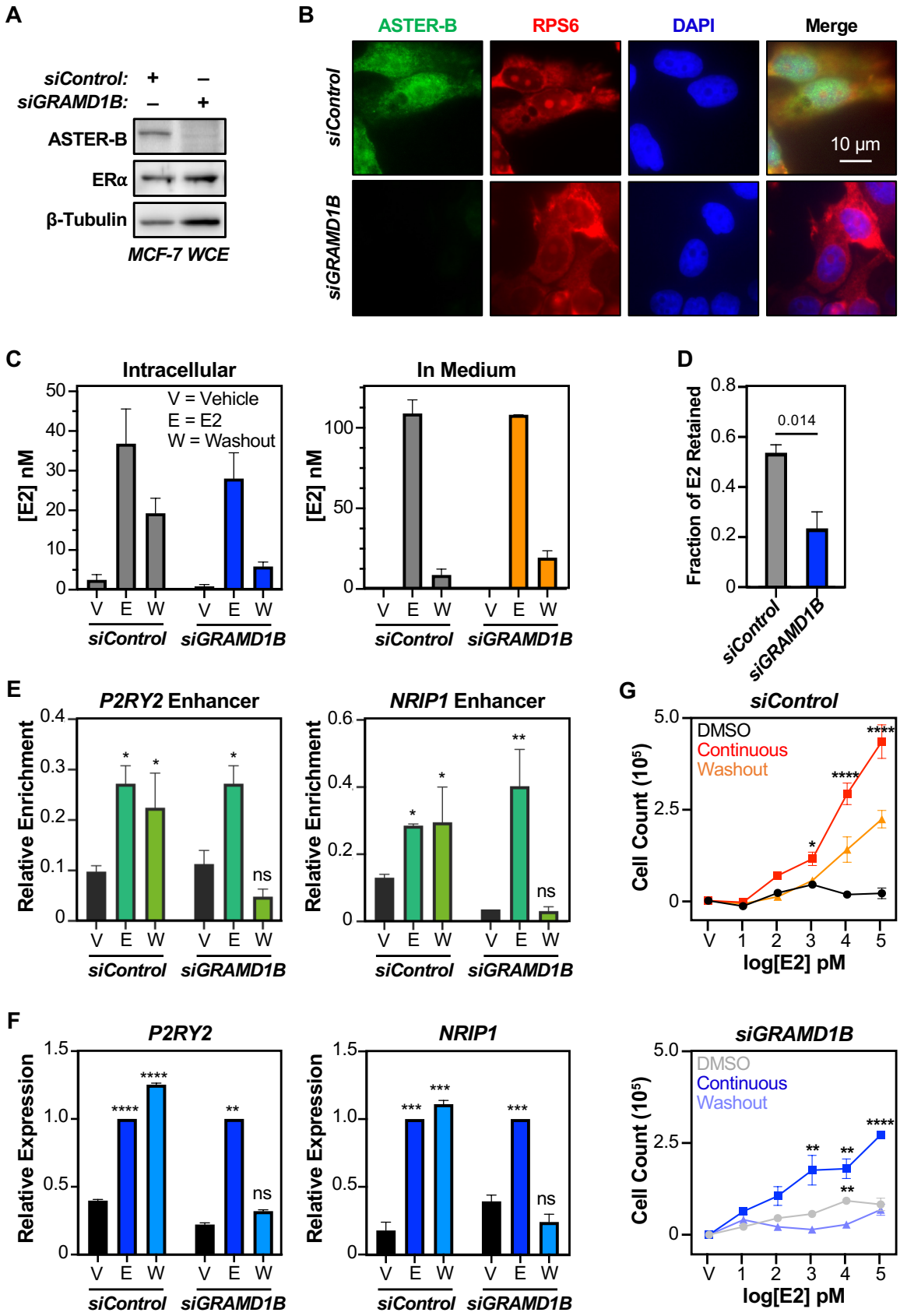

Kim and Kraus (2024) - Figure 6

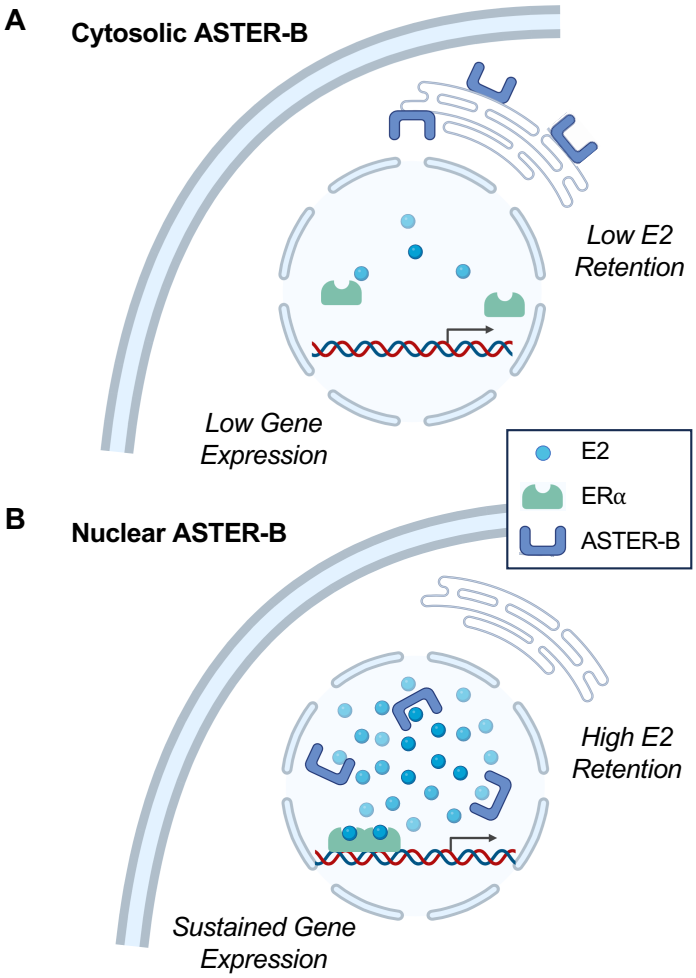

Kim and Kraus (2024) - Figure 7